Figures and figure supplements

YAP/TAZ enhances P-body formation to promote tumorigenesis

Xia Shen, Xiang Peng and YueGui Guo *et al*.

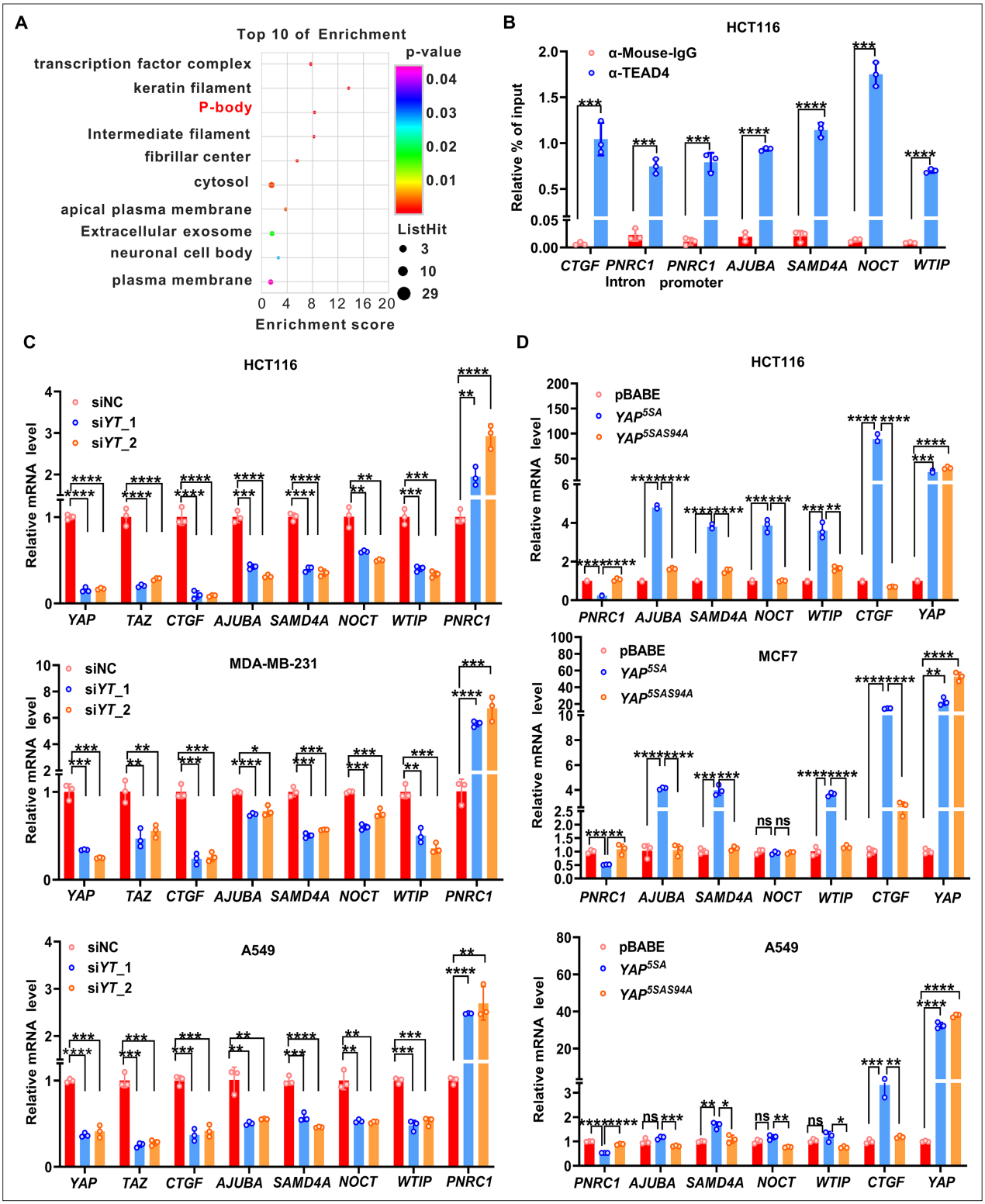

Figure 1. YAP/TAZ transcriptionally regulates genes related to P-bodies. (**A**) Gene Ontology (GO) analysis of the downregulated genes upon knockdown of *YAP/TAZ* in HCT116 cells. The graph shows enrichment in the cellular component category. (**B**) ChIP–qPCR analysis of endogenous TEAD4 binding to the genomic locus of the indicated P-body-related genes in HCT116 cells. The *CTGF* promoter was included as the positive control. (**C**) qPCR analysis of the mRNA levels of the indicated P-body-related genes in *YAP/TAZ* knockdown HCT116, MDA-MB-231, and A549 cells. Cells were transfected with *YAP/TAZ* siRNA for 3 d before qPCR analysis. (**D**) qPCR analysis of the mRNA levels of the indicated P-body-related genes in HCT116, MCF7, and A549 cells stably expressing YAP^{5SA} and $YAP^{5SA\text{-}S94A}$. Cells were infected with *YAP^{5SA}*- and *$YAP^{5SA\text{-}S94A}$*-containing retroviruses and selected with

Figure 1 continued on next page

Figure 1 continued

puromycin for 1 wk before qPCR analysis. n = 3 biologically independent samples per group. Two-tailed Student's *t*-test (**B**) and one-way ANOVA (**C, D**) were performed to assess statistical significance in this figure. These data (**B–D**) are representative of three independent experiments.

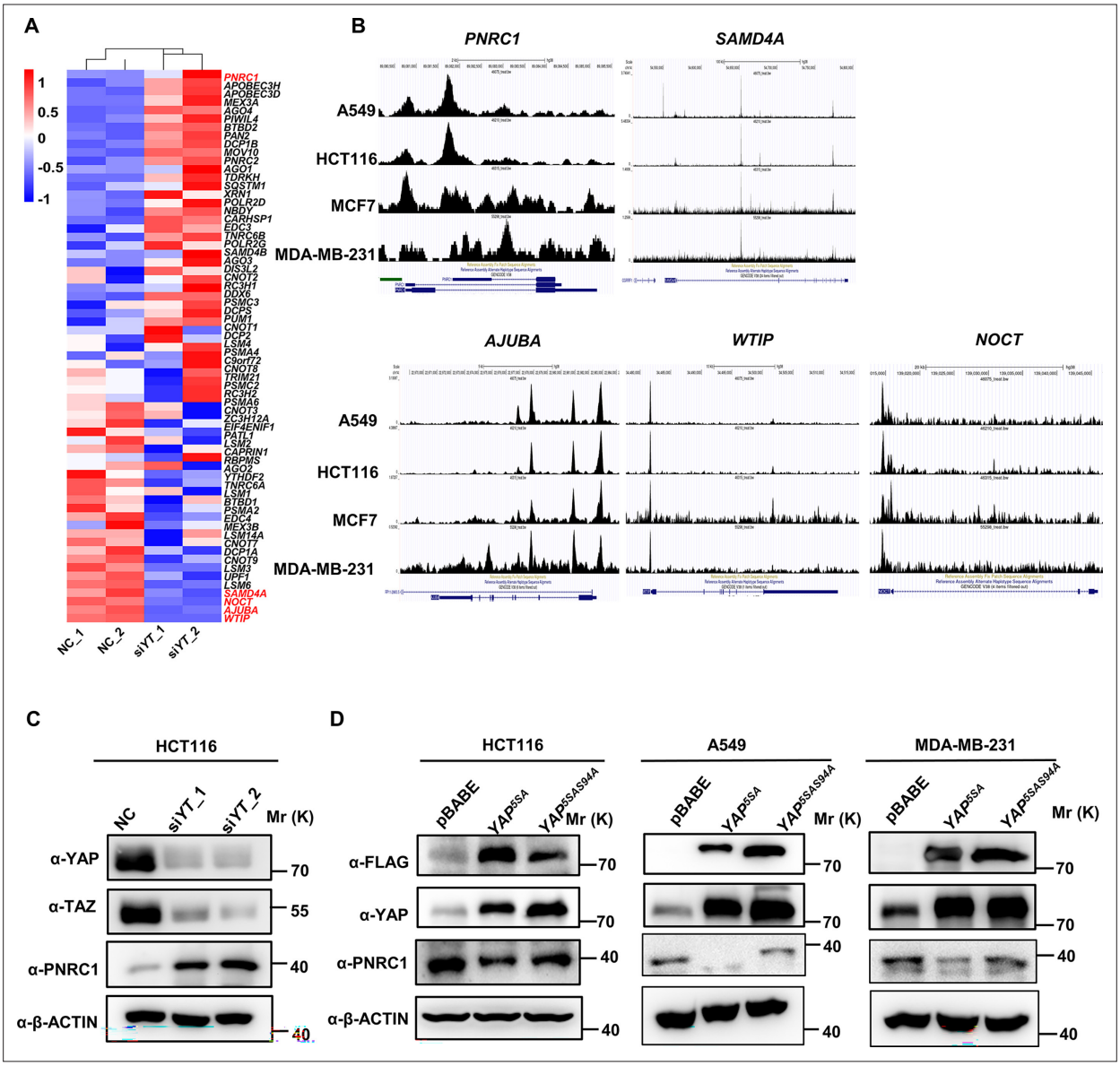

Figure 1—figure supplement 1. RNA-seq and ChIP-seq analysis of YAP/TEAD's target genes related to P-bodies. (**A**) Heatmap showing the mRNA levels of 76 genes annotated as P-body-related genes, as detected in HCT116 cells by RNA-seq (GSE176475). (**B**) Representative sequencing TEAD4 ChIP-seq tracks at the *SAMD4A/AJUBA/WTIP/NCOT/PNRC1* loci in HCT-116, A549, MDA-MB-231, and MCF7 cells. The ChIP-seq data were extracted from the Cistrome database and uploaded to the UCSC Genome Browser for visualization. (**C**) Western blot analysis of PNRC1, YAP, and TAZ in control and *YAP/TAZ* knockdown HCT116 cells. (**D**) Western blot analysis of PNRC1, YAP, and FLAG in control HCT116 cells and HCT116 cells overexpressing FLAG-YAP^{5SA} and YAP$^{5SA\text{-}S94A}$. These data (**C, D**) are representative of two independent experiments.

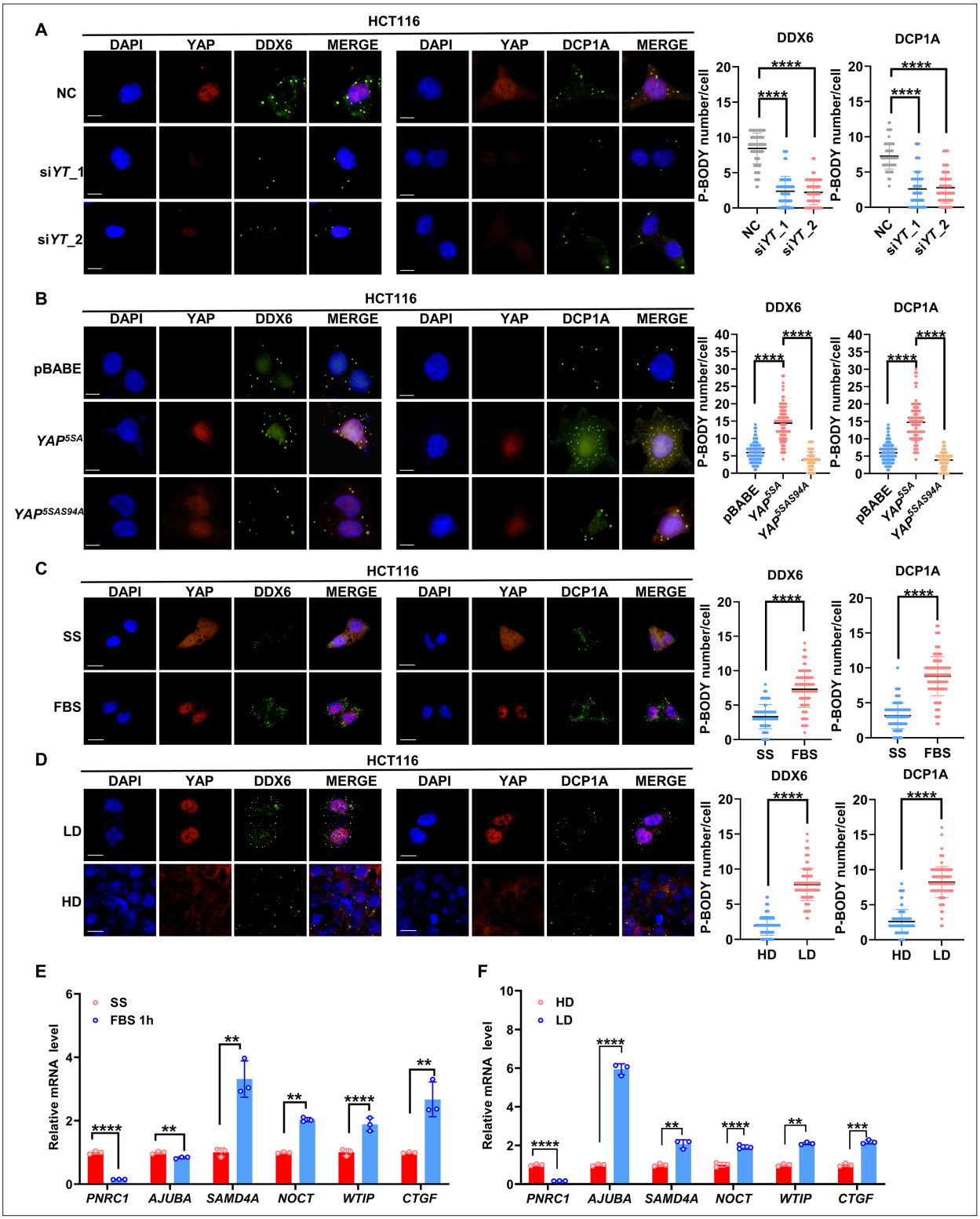

Figure 2. YAP/TAZ promotes P-body formation in colorectal cancer (CRC) cells. (**A**) Immunofluorescence analysis of the P-body markers DDX6 and DCP1A in *YAP/TAZ* knockdown HCT116 cells. Cells were transfected with *YAP/TAZ* siRNA for 3 d before processing for immunofluorescence staining using anti-DDX6 and anti-DCP1A antibodies. Foci were counted in 100 cells per group. (**B**) Immunofluorescence analysis of DDX6 and DCP1A in HCT116 cells expressing YAP^{5SA} and $YAP^{5SA\text{-}S94A}$. (**C**) Immunofluorescence analysis of DDX6 and DCP1A in HCT116 cells. Cells were treated with 10% fetal bovine serum (FBS) for 1 hr after overnight serum starvation (SS). (**D**) Immunofluorescence analysis of DDX6 and DCP1A in HCT116 cells in sparse or confluent culture. (**E, F**) qPCR analysis of the indicated genes in HCT116 cells. HCT116 cells were treated with 10% FBS for 1 hr after overnight SD (**E**) or culture

Figure 2 continued on next page

Figure 2 continued

under sparse or confluent conditions in standard culture medium (**F**). Kruskal–Wallis test (**A, B**), Mann–Whitney *U* test (**C, D**), and two-tailed Student's *t*-test (**E, F**) were performed to assess statistical significance. These data (**A–F**) are representative of three independent experiments.

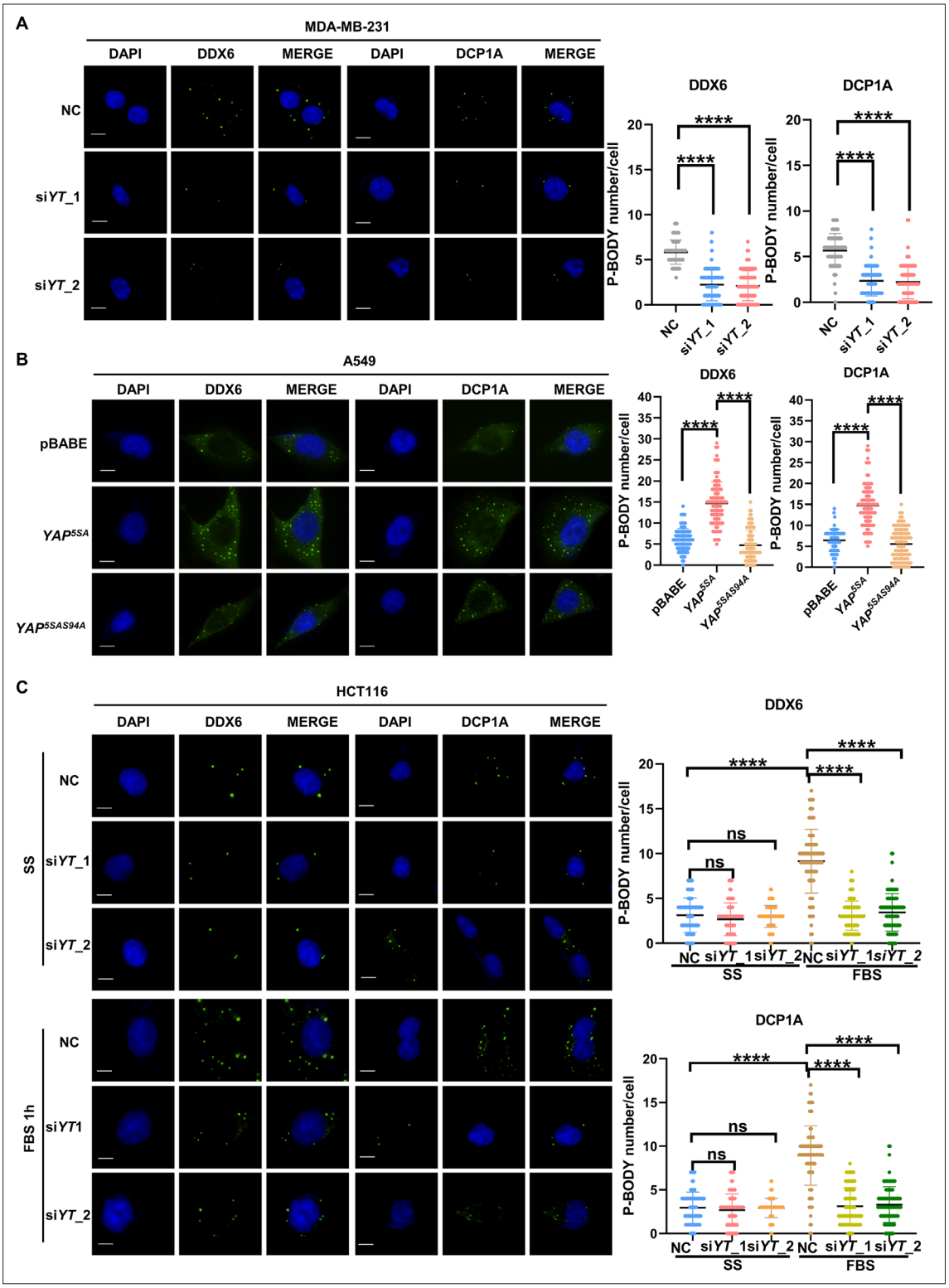

Figure 2—figure supplement 1. YAP/TAZ modulates P-body formation in breast, lung and colorectal cancer cells. (**A**) Immunofluorescence analysis of the P-body markers DDX6 and DCP1A in *YAP/TAZ* knockdown MDA-MB-231 cells. Cells were transfected with *YAP/TAZ* siRNA for 3 d before processing for immunofluorescence staining using anti-DDX6 and anti-DCP1A antibodies. Foci were counted in 100 cells per group. (**B**) Immunofluorescence analysis of DDX6 and DCP1A in A549 cells expressing YAP^{5SA} and $YAP^{5SA\text{-}S94A}$. (**C**) Immunofluorescence analysis of DDX6 and DCP1A in HCT116 cells. Cells were transfected with control and *YAP/TAZ* siRNA for 3 d before overnight serum starvation. Then, the starved cells were treated with 10% fetal bovine serum (FBS) for 1 hr before immunofluorescence staining. Kruskal–Wallis test was performed to assess statistical significance. These data (**A–C**) are representative of three independent experiments.

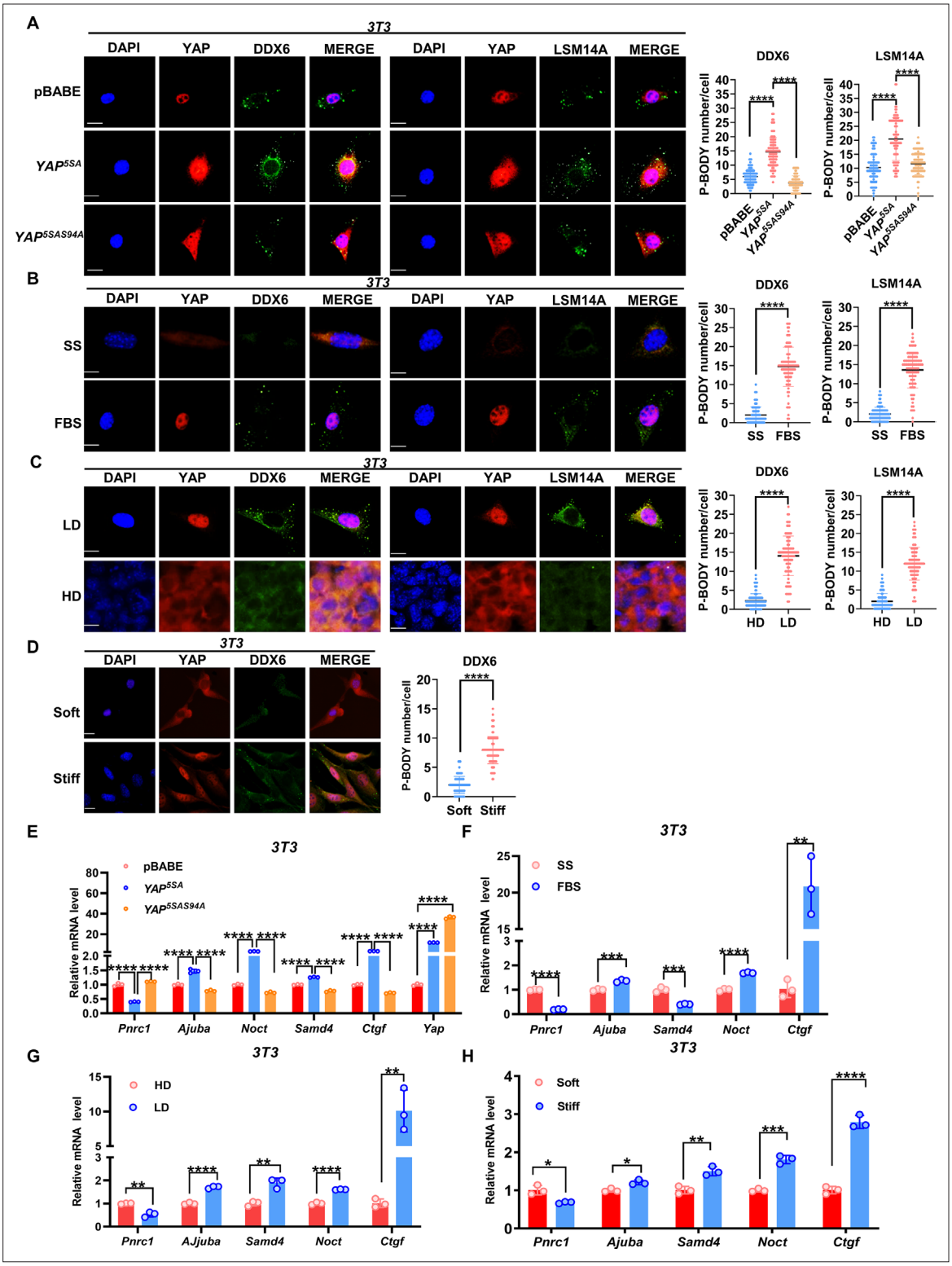

Figure 2—figure supplement 2. YAP/TAZ modulates P-body formation in untransformed NIH3T3 cells. (**A**) Immunofluorescence analysis of DDX6 and LSM14A in NIH3T3 cells expressing YAP^{5SA} and YAP$^{5SA\text{-}S94A}$. Foci were counted in 100 cells per group. (**B**) Immunofluorescence analysis of DDX6 and LSM14A in NIH3T3 cells. Sparse cells were treated with 10% fetal bovine serum (FBS) for 1 hr after overnight serum starvation (SS). (**C**) Immunofluorescence analysis of DDX6 and LSM14A in NIH3T3 cells in sparse or confluent culture. (**D**) Immunofluorescence analysis of DDX6 and LSM14A in NIH3T3 cells cultured on soft (1 kPa) to stiff (40 kPa) matrices. (**E–H**) qPCR analysis of the indicated genes in NIH3T3 cells expressing YAP^{5SA} and YAP$^{5SA\text{-}S94A}$ (**E**) or NIH3T3 cells treated with 10% FBS for 1 hr after overnight SS (**F**) or cultured under sparse or confluent conditions in standard

Figure 2—figure supplement 2 continued on next page

Figure 2—figure supplement 2 continued

culture medium (**G**) or cultured on soft (1 kPa) to stiff (40 kPa) matrices (**H**). Kruskal–Wallis test (**A**), Mann–Whitney *U* test (**B–D**), one-way ANOVA (**E**), and two-tailed Student's *t*-test (**F–H**) were performed to assess statistical significance. These data (**A–H**) are representative of three independent experiments.

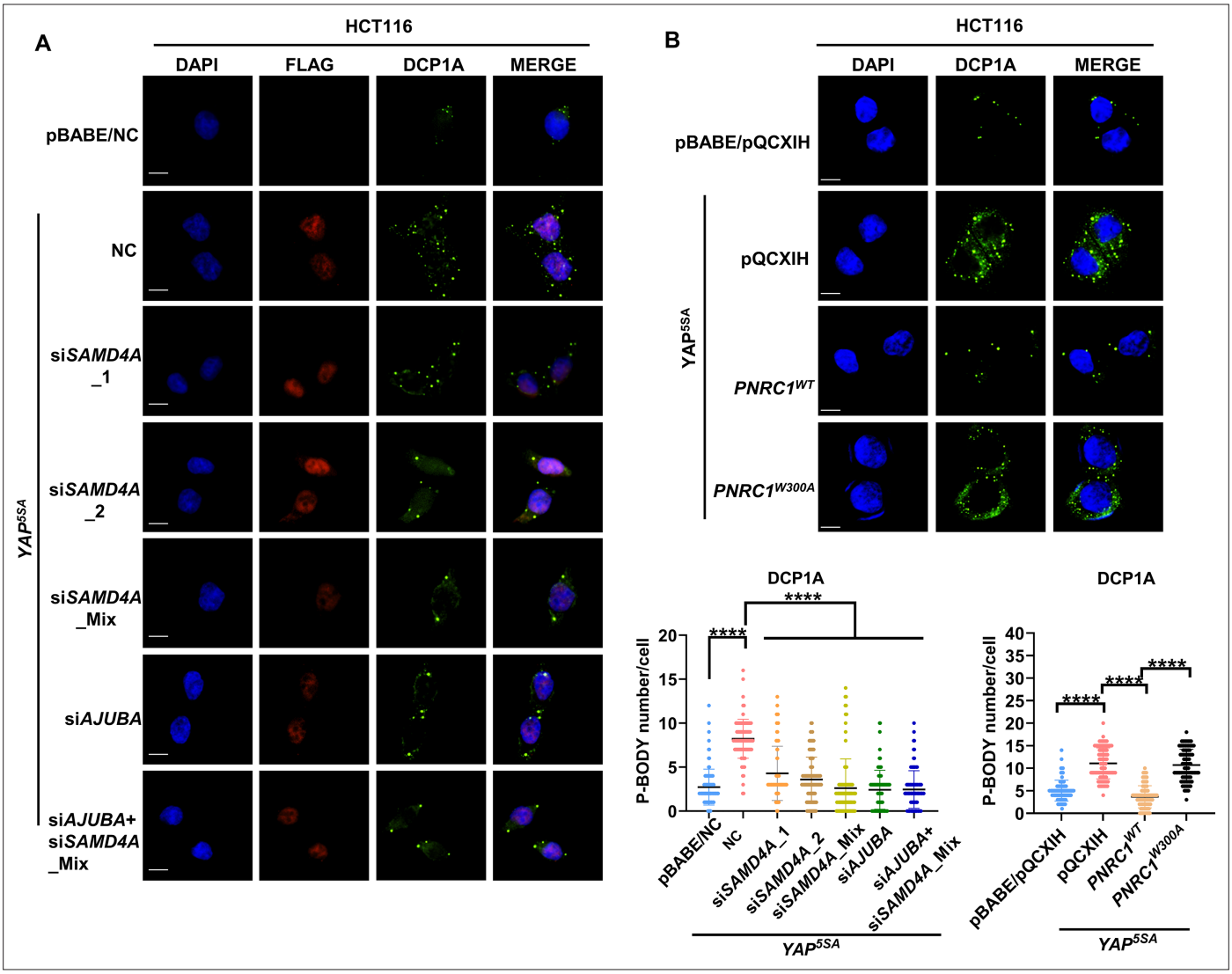

Figure 3. SAMD4A, AJUBA, and PNRC1 mediate the regulatory functions of YAP/TAZ in P-body formation. (**A**) Immunofluorescence analysis of DDX6 and DCP1A in HCT116 cells stably expressing YAP^{5SA} and YAP^{5SA}-expressing cells transiently transfected with *SMAD4A* and *AJUBA* siRNA. Foci were counted in 100 cells per group. (**B**) Immunofluorescence analysis of DDX6 and DCP1A in HCT116 cells expressing YAP^{5SA} alone or in combination with PNRC1^{WT} or PNRC1^{W300A}. Kruskal–Wallis test was performed to assess statistical significance. These data (**A–B**) are representative of three independent experiments.

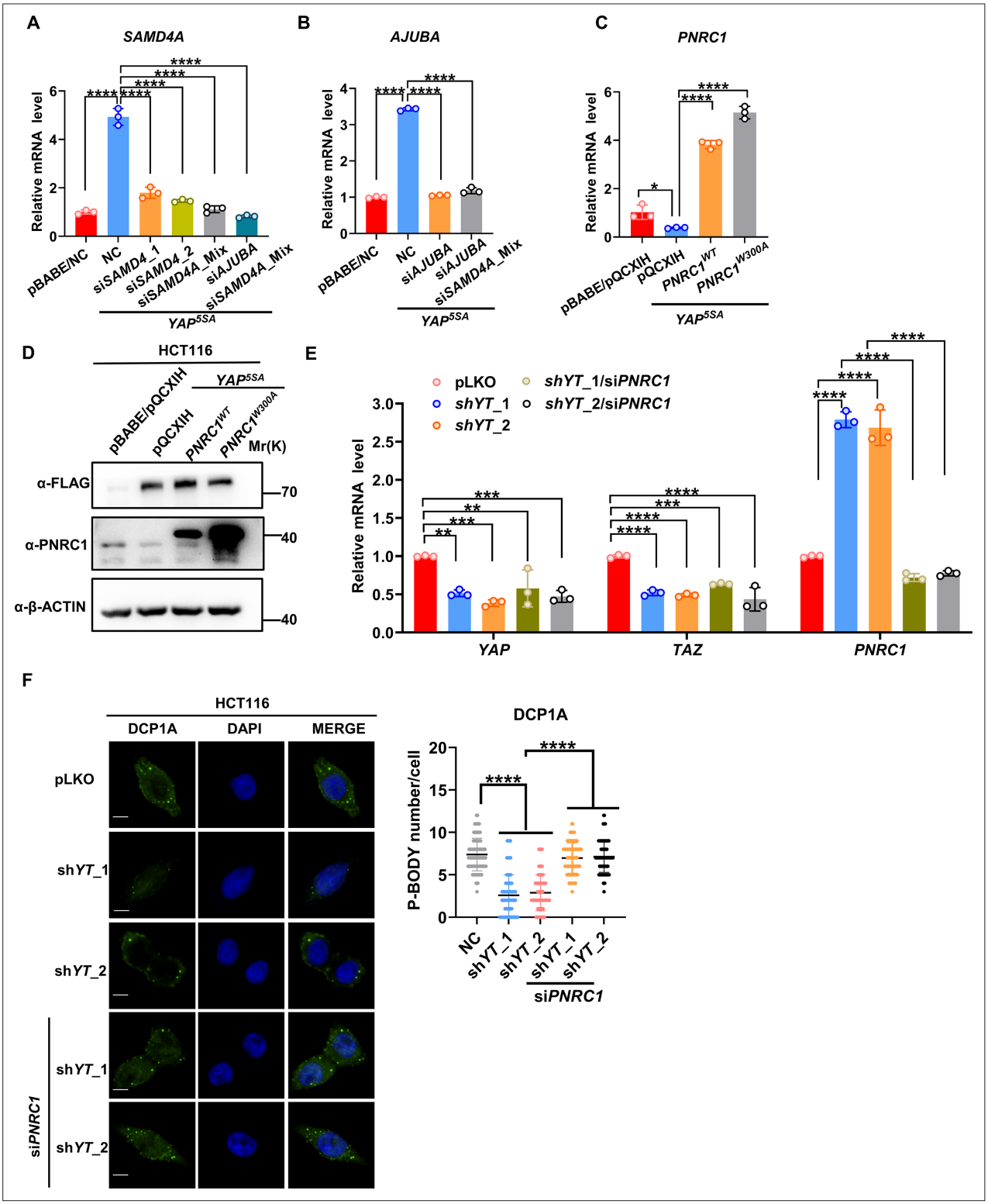

Figure 3—figure supplement 1. Knockdown of *PNRC1* reverses the attenuated P-body formation induced by *YAP/TAZ* knockdown. (**A, B**) qPCR analysis of the mRNA levels of *SAMD4A* (**A**) and *AJUBA* (**B**) in HCT116 cells stably expressing FLAG-YAP^{5SA} and YAP^{5SA} and transfected with *SMAD4A* or *AJUBA* siRNA. n = 3 biologically independent samples per group. (**C, D**) qPCR (**C**) and western blot (**D**) analysis of PNRC1 expression in HCT116 cells stably expressing FLAG-YAP^{5SA} alone or in combination with PNRC1^{WT} or PNRC1^{W300A}. (**E**) qPCR analysis of the mRNA level of *PNRC1/YAP/TAZ* in *YAP/TAZ* knockdown HCT116 cells transfected with PNRC1 siRNA. n = 3 biologically independent samples per group. (**F**) Immunofluorescence analysis of DCP1A in *YAP/TAZ* knockdown HCT116 cells transfected with *PNRC1* siRNA. Foci were counted in 100 cells per group. One-way ANOVA (**A–C, E**) and

Figure 3—figure supplement 1 continued on next page

Figure 3—figure supplement 1 continued

Kruskal–Wallis test (**F**) were performed to assess statistical significance for qPCR analysis in this figure. The data (**F**) is representative of two independent experiments.

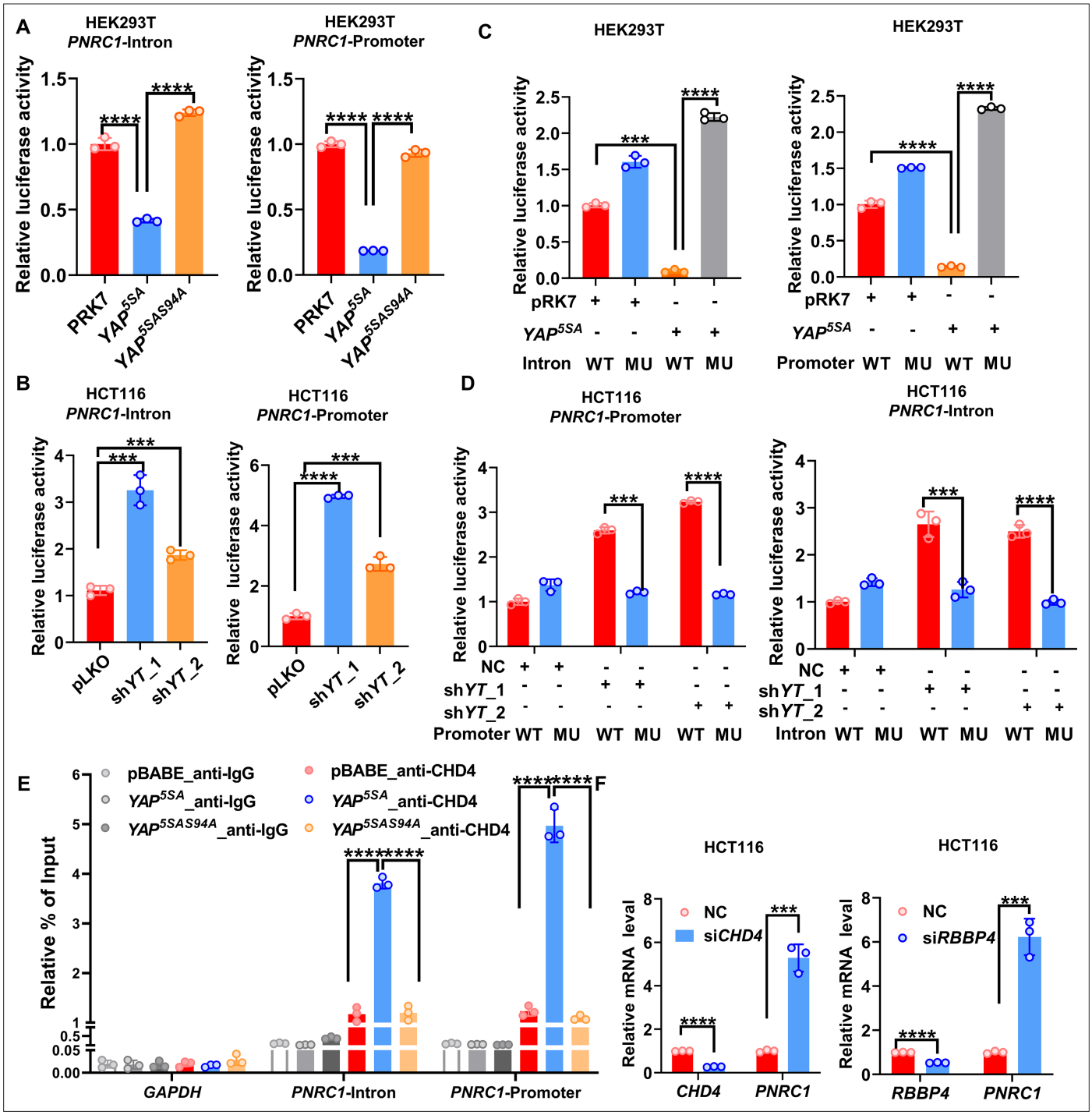

Figure 4. YAP suppresses PNRC1 gene transcription by recruiting the NuRD complex. (**A**) Overexpression of YAP^{5SA} but not YAP$^{5SA\text{-}S94A}$ decreased the luciferase activity of the *PNRC1* promoter and intron reporters. HEK-293T cells were transfected with the indicated FLAG-*YAP*^{5SA} and *YAP*$^{5SA\text{-}S94A}$ expression plasmids and the *PNRC1* promoter or intron luciferase reporter. (**B**) Knockdown of *YAP/TAZ* stimulated the luciferase activity of the *PNRC1* promoter and intron reporters. The *PNRC1* promoter or intron luciferase reporter plasmid and the Renilla luciferase reporter plasmid were co-transfected into HCT116 cells stably expressing pLKO-vec, sh*YAP/TAZ*-1, or sh*YAP/TAZ*-2. (**C, D**) Luciferase assay of the *PNRC1* promoter/intron WT reporters and mutant reporters with TEAD binding motif mutations in HEK-293T cells (**C**) and HCT116 cells (**D**). (**E**) ChIP–qPCR analysis of CHD4 binding to the *PNRC1* promoter and intronic regions in control and HCT116 cells stably expressing FLAG-YAP^{5SA} or YAP$^{5SA\text{-}S94A}$. (**F**) qPCR analysis of *PNRC1*, *CHD4*, and *RBBP4* in HCT116 cells transfected with the indicated siRNAs. n = 3 biologically independent samples per group. One-way ANOVA (**A–E**) and two-tailed Student's *t*-test (**F**) were performed to assess statistical significance in this figure. These data (**A–F**) are representative of two independent experiments.

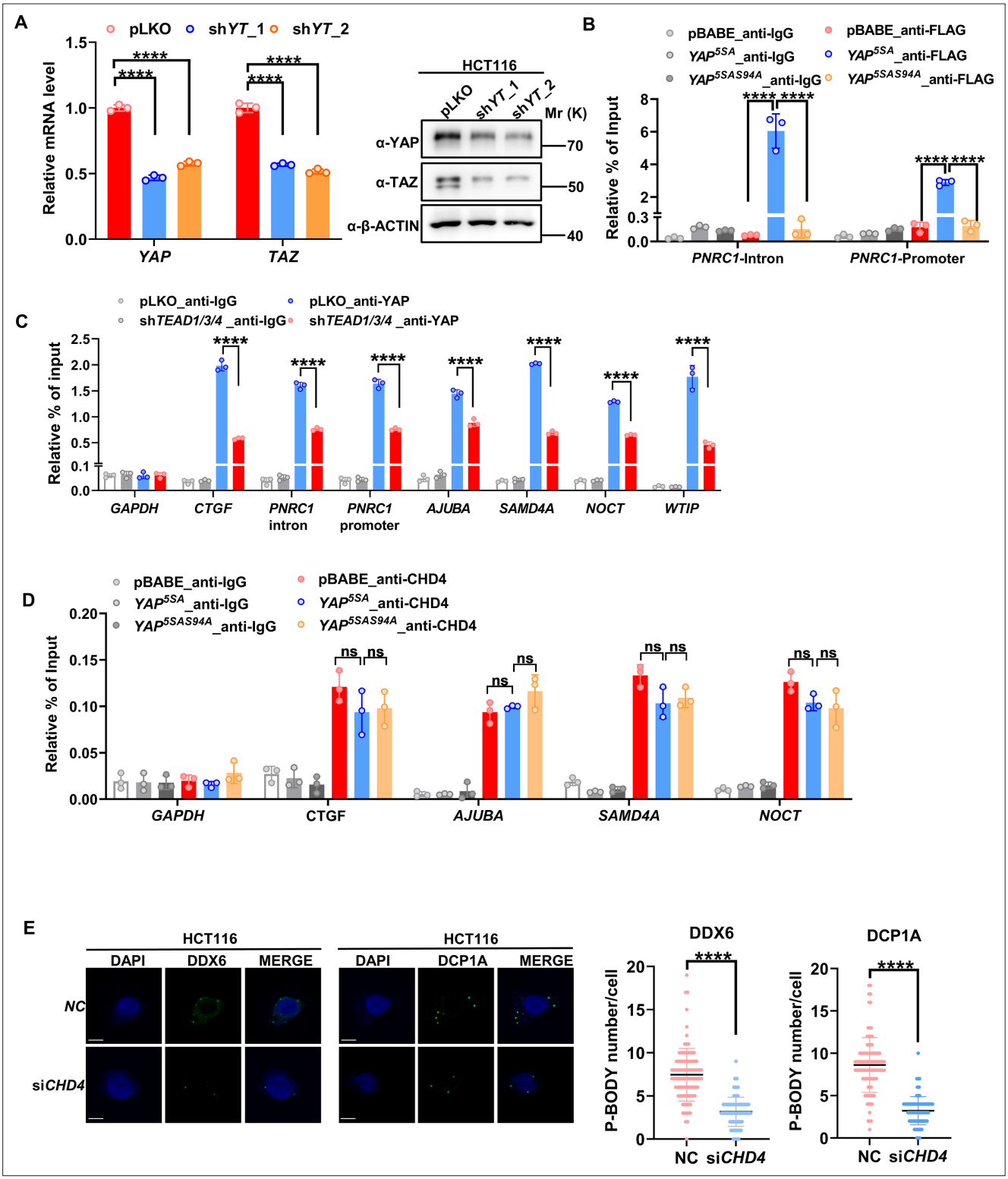

Figure 4—figure supplement 1. TEADs and CHD4 mediates YAP-dependent inhibition on *PNRC1* gene transcription. (**A**) qPCR and western blot analysis of the YAP/TAZ knockdown stable HCT116 cells. (**B**) ChIP–qPCR analysis of FLAG-YAP^{5SA}, YAP$^{5SA\text{-}S94A}$ binding to the *PNRC1* promoter and intronic regions in control and HCT116 cells stably expressing FLAG-YAP^{5SA} or YAP$^{5SA\text{-}S94A}$. (**C**) ChIP–qPCR analysis of YAP binding to the genomic locus of the indicated P-body-related genes in control and HCT116 cells with stably knockdown of *TEAD1/3/4*. (**D**) ChIP–qPCR analysis of CHD4 binding to the YAP binding sites of indicated genes in control and HCT116 cells stably expressing FLAG-YAP^{5SA} or YAP$^{5SA\text{-}S94A}$. One-way ANOVA was performed to assess statistical significance for qPCR analysis in this figure. These data (**B–D**) are representative of two independent experiments. (**E**) Immunofluorescence

Figure 4—figure supplement 1 continued on next page

Figure 4—figure supplement 1 continued

analysis of DDX6 and DCP1A in HCT116 cells. Cells were transfected with control and *CHD4* siRNA for 3 d before Immunofluorescence analysis. Foci were counted in 100 cells per group. Kruskal–Wallis test was performed to assess statistical significance.

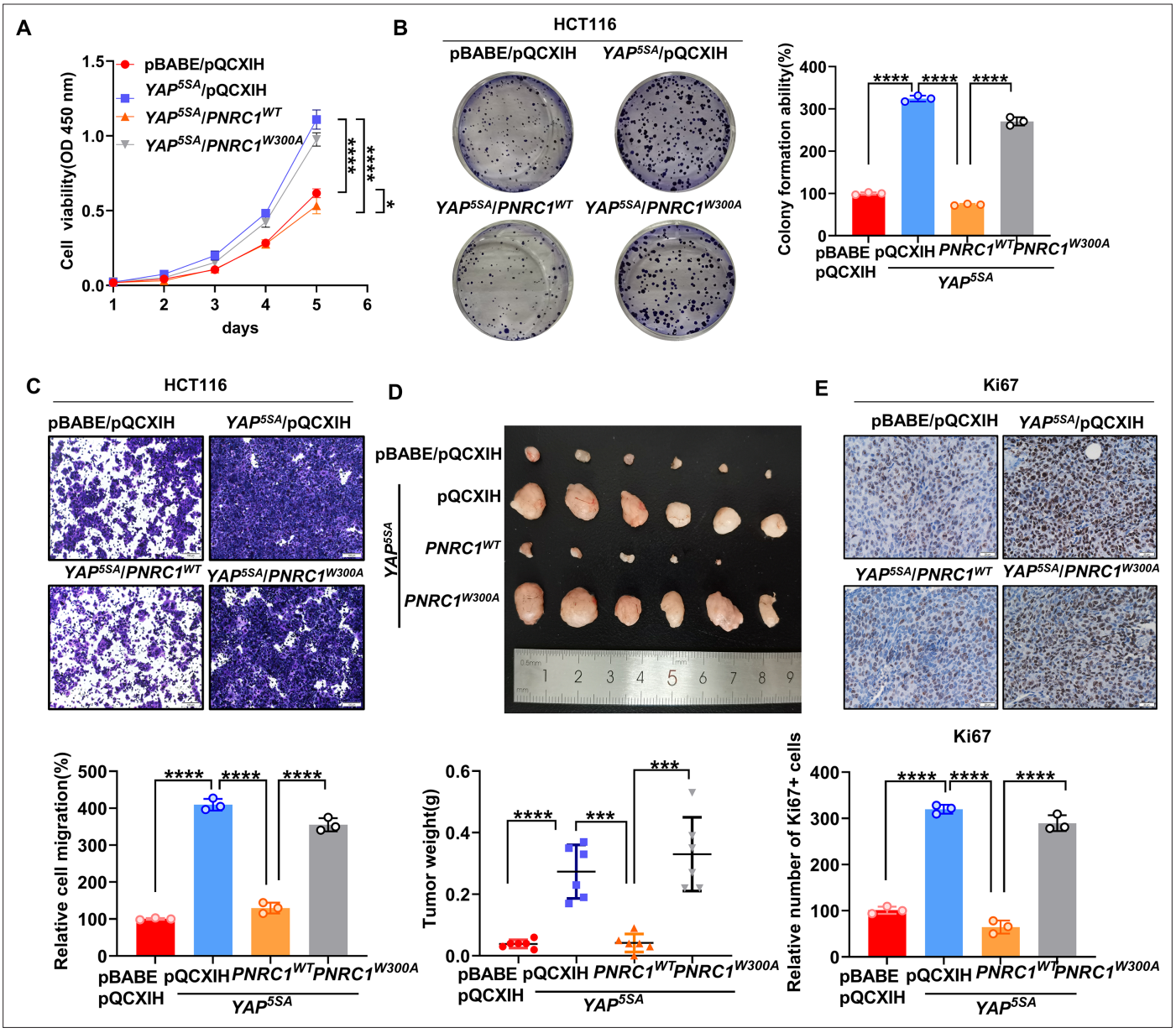

Figure 5. PNRC1 attenuates the oncogenic function of YAP in colorectal cancer (CRC). (**A**) CCK8 proliferation assays of HCT116 cells stably expressing YAP^{5SA} alone or in combination with of PNRC1^{WT} or PNRC1^{W300A}. n = 4 biologically independent samples per group. (**B, C**) Colony formation assay (**B**) and Transwell assay (**C**) of HCT116 cells stably expressing YAP^{5SA} alone or in combination with PNRC1^{WT} or PNRC1^{W300A}. n = 3 biologically independent samples per group. (**D**) Representative images of xenograft tumors formed from HCT116 cells stably expressing YAP5SA alone or in combination with of PNRC1^{WT} or PNRC1^{W300A} (n = 6). (**E**) Representative images of IHC staining of the proliferation marker Ki67 in xenograft tumors formed from HCT-116 cells stably expressing YAP^{5SA} alone or in combination with PNRC1^{WT} or PNRC1^{W300A} (n = 3). Two-way ANOVA (**A**) and one-way ANOVA (**B–E**) were performed to assess statistical significance in this figure. These data (**A–C**) are representative of two independent experiments.

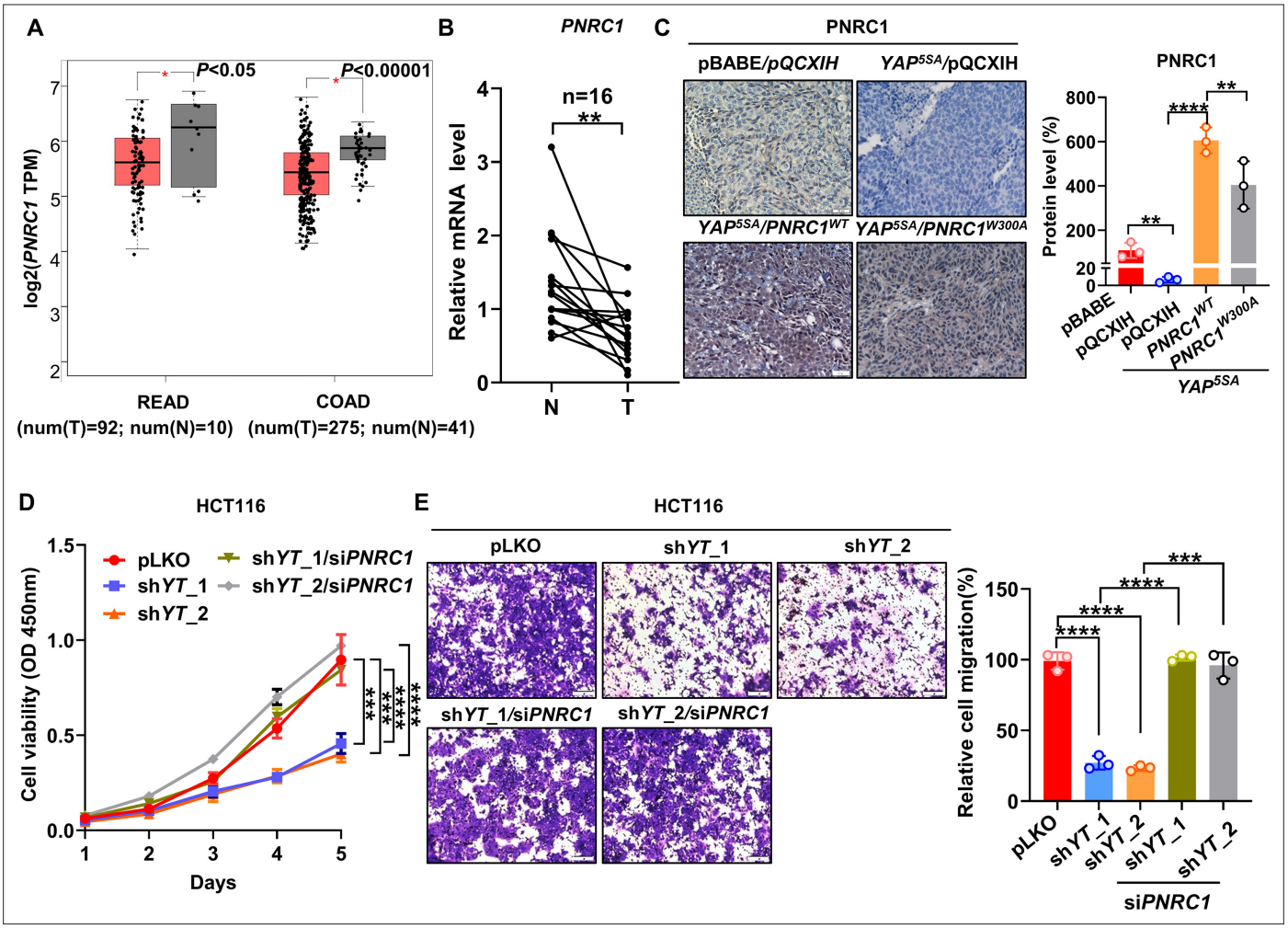

Figure 5—figure supplement 1. *PNRC1* is a tumor suppressor gene in CRC. (**A**) Downregulated mRNA expression of PNRC1 in colon cancer (COAD) and rectal cancer (READ) colorectal cancer (CRC) datasets in TCGA. The mRNA levels of *PNRC1* were extracted from the GEPIA database. (**B**) qPCR analysis of the mRNA levels of *PNRC1* in 16 paired normal mucosa and colorectal tumor tissues. Paired Student's *t*-test was performed to assess statistical significance. (**C**) Representative images of IHC staining of PNRC1 in xenograft tumors formed from HCT116 cells stably expressing YAP^{5SA} alone or in combination with $PNRC1^{WT}$ or $PNRC1^{W300A}$ (n = 3). (**D, E**) CCK8 proliferation assay (n = 4) (**D**) and Transwell migration assay (n = 3) (**E**) of YAP/TAZ knockdown HCT116 cells transfected with *PNRC1* siRNA. One-way ANOVA (**A, C, E**) and two-way ANOVA (**D**) were performed to assess statistical significance. These data (**D, E**) are representative of three independent experiments.

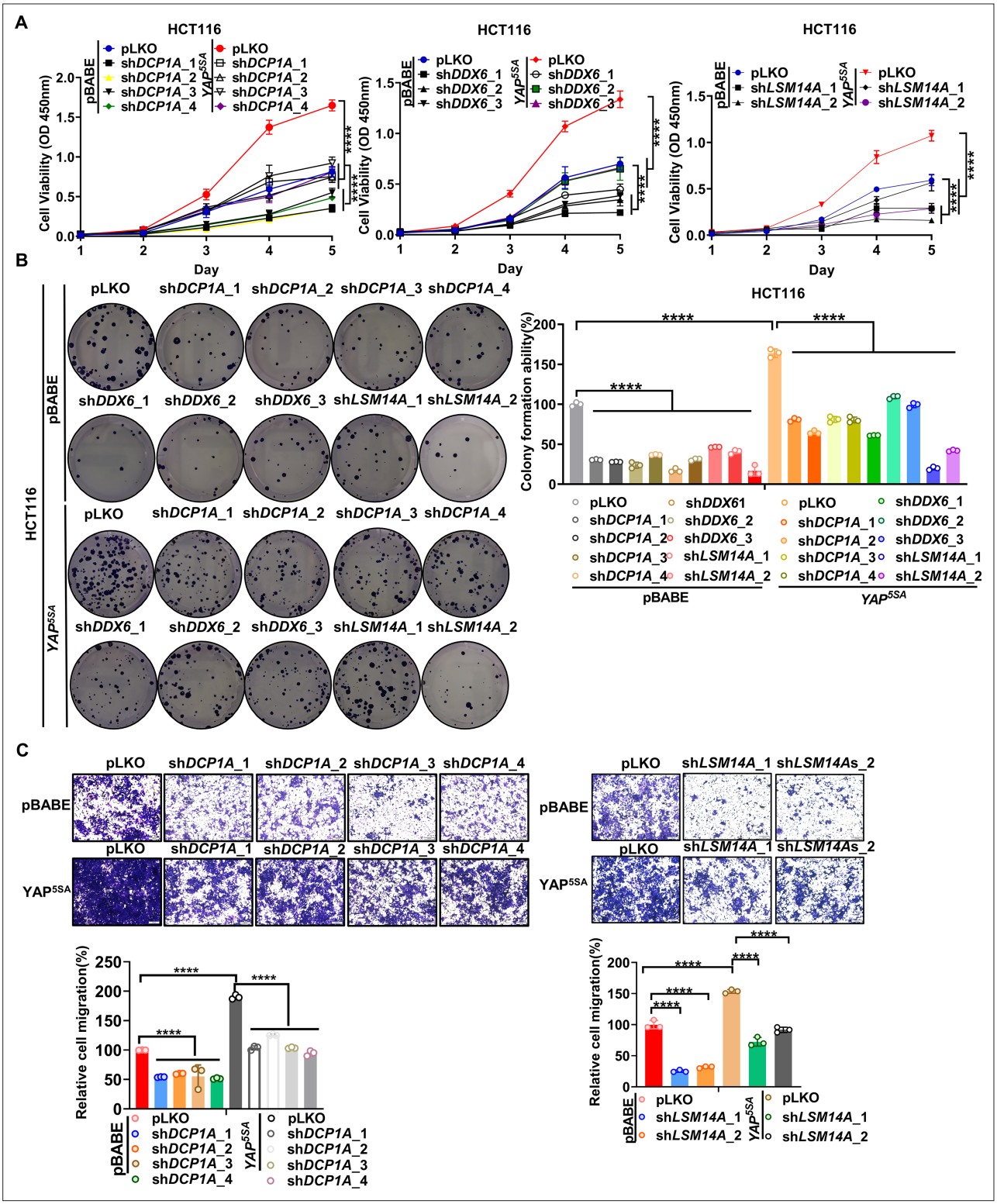

Figure 6. Knockdown of P-body-related core genes suppresses the oncogenic function of YAP in colorectal cancer (CRC). (**A**) CCK8 proliferation assays of control HCT116 cells with or without knockdown of *DCP1A*, *LSM14A* or *DDX6* and HCT116 cells stably expressing YAP^{5SA} with or without knockdown of *DCP1A*, *LSM14A*, or *DDX6*. n = 5 biologically independent samples per group. (**B, C**) Colony formation assay (**B**) and Transwell assay (**C**) of control HCT116 cells with or without knockdown of *DCP1A*, *LSM14A*, or *DDX6* and HCT116 cells stably expressing YAP^{5SA} with or without knockdown of *DCP1A*, *LSM14A*, or *DDX6*. n = 3 biologically independent samples per group. Two-way ANOVA (**A**) and one-way ANOVA (**B, C**) were performed to assess statistical significance in this figure. These data (**A–C**) are representative of three independent experiments.

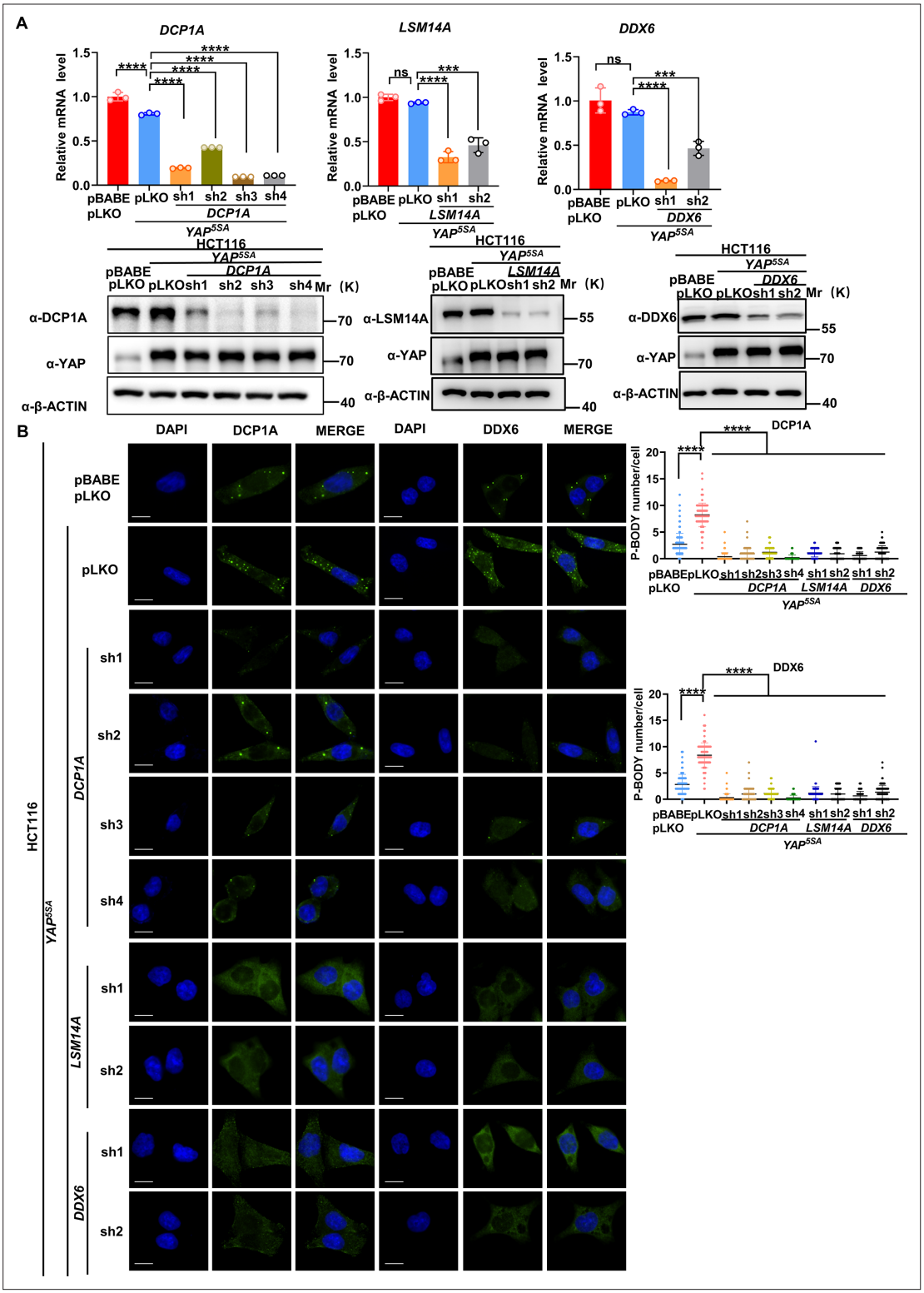

Figure 6—figure supplement 1. Knockdown efficiency and P-body reduction in *DCP1A/LSM14A/DDX6* knockdown HCT116 cells. (**A**) qPCR and western blot analysis of the knockdown efficiency of *DCP1A*, *LSM14A*, and *DDX6* in HCT116 cells stably expressing YAP^{5SA} with or without knockdown of *DCP1A*, *LSM14A*, or *DDX6*. n = 3 biologically independent samples per group. (**B**) Immunofluorescence analysis of DDX6 and DCP1A in HCT116 cells stably expressing YAP^{5SA} with or without knockdown of *DCP1A*, *LSM14A*, or *DDX6*. Foci were counted in 100 cells per group. One-way ANOVA (**A**) and Kruskal–Wallis test (**B**) were performed to assess statistical significance.

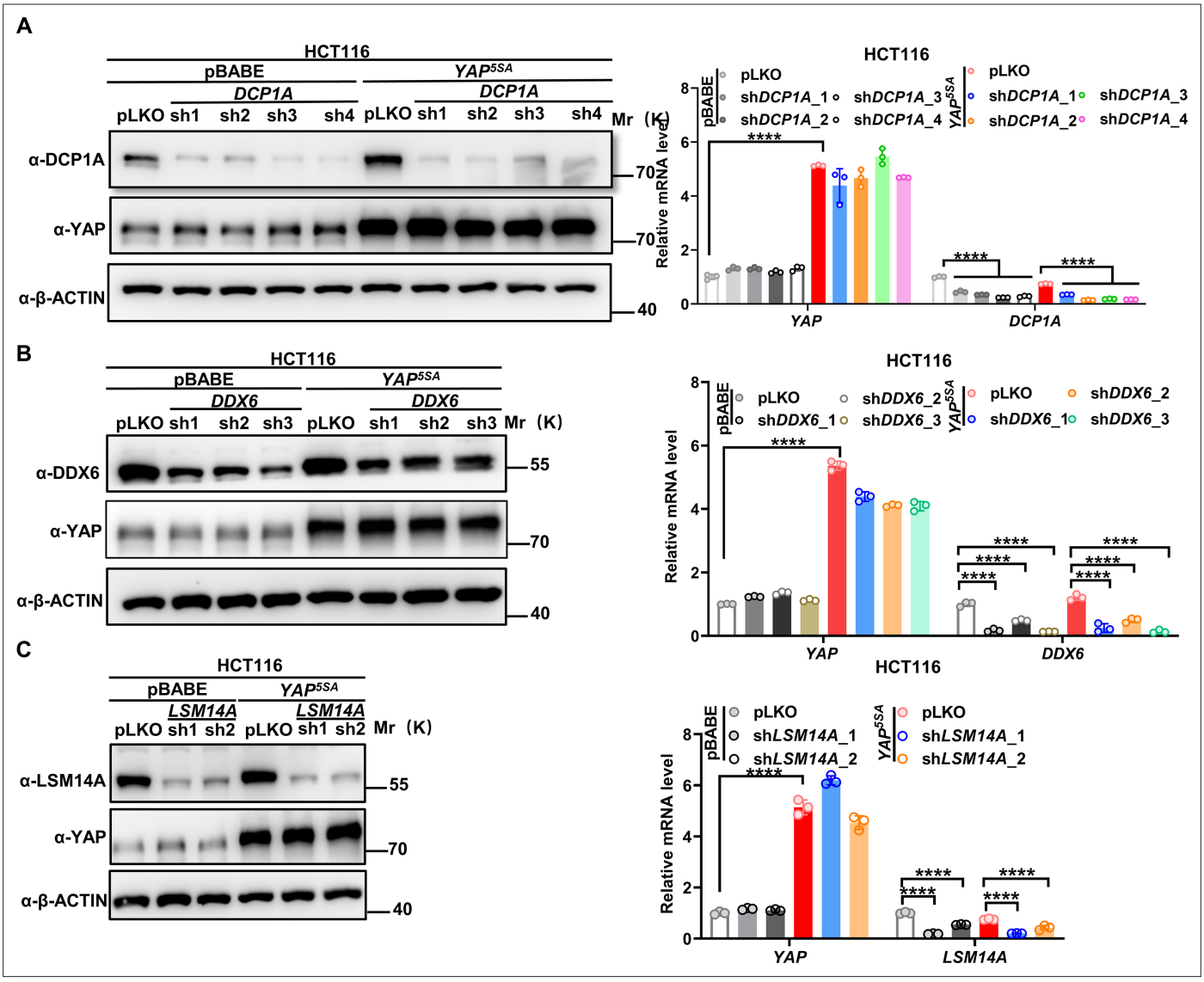

Figure 6—figure supplement 2. Confirmation of *DCP1A/ LSM14A/DDX6* knockdown in YAP^{5SA}-expressing HCT116 cells. (**A–C**) qPCR and western blot analysis of the knockdown efficiency of *DCP1A* (**A**), *DDX6* (**B**), and *LSM14A* (**C**) in control HCT116 cells with or without knockdown of *DCP1A*, *LSM14A*, or *DDX6* and stable YAP^{5SA} overexpression HCT116 cells with or without knockdown of *DCP1A*, *LSM14A*, or *DDX6*. n = 3 biologically independent samples per group. One-way ANOVA was performed to assess statistical significance.

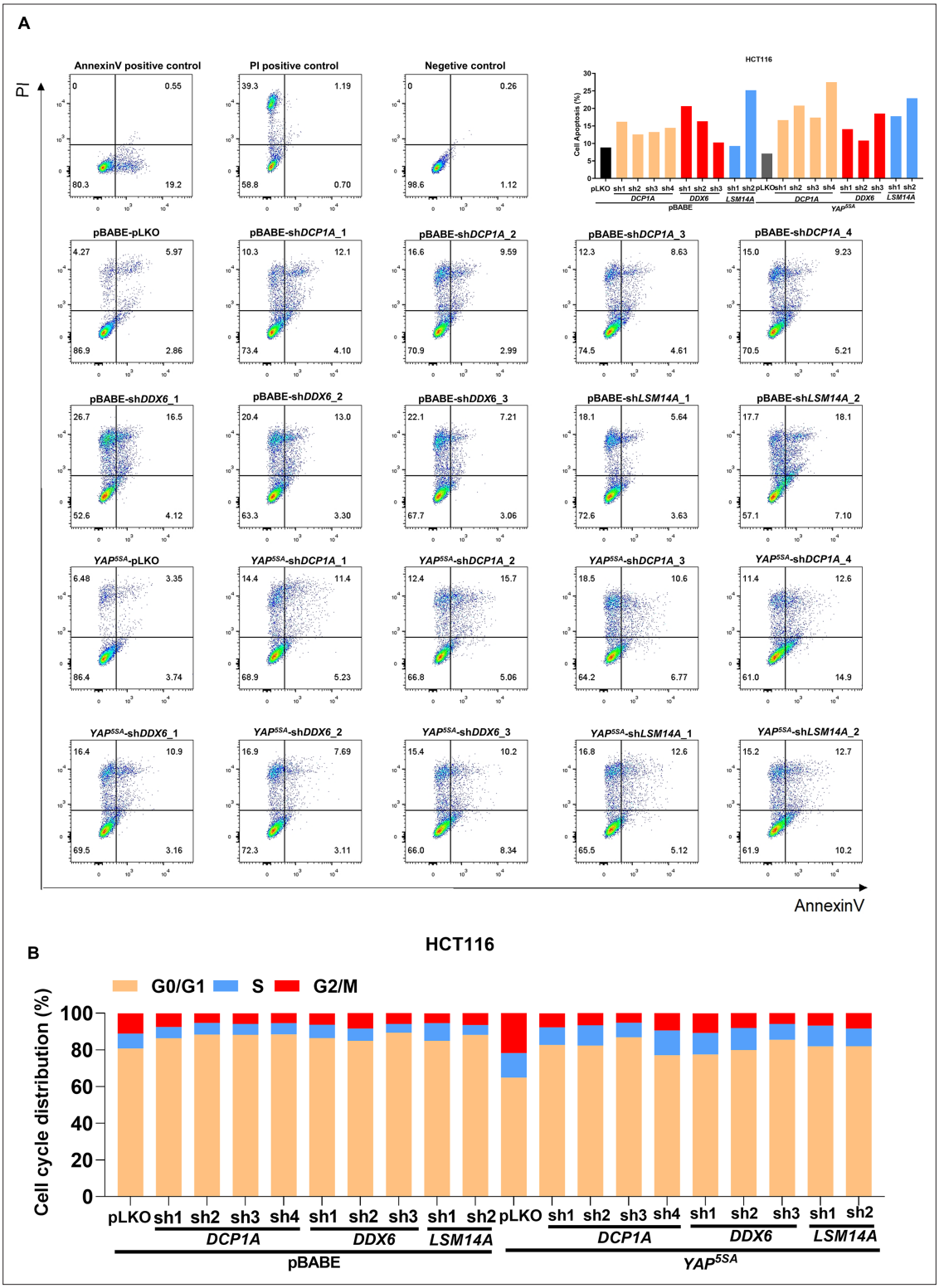

Figure 6—figure supplement 3. Knockdown of *DCP1A, LSM14A* and *DDX6* downregulates cell mitosis and increases cell apoptosis in YAP^{5SA}-expressing HCT116 cells. (**A, B**) Cell apoptosis (**A**) and cell cycle (**B**) analysis of the control HCT116 cells with or without knockdown of *DCP1A*, *LSM14A*, or *DDX6* and stable YAP^{5SA} overexpression HCT116 cells with or without knockdown of *DCP1A, LSM14A, or DDX6*.

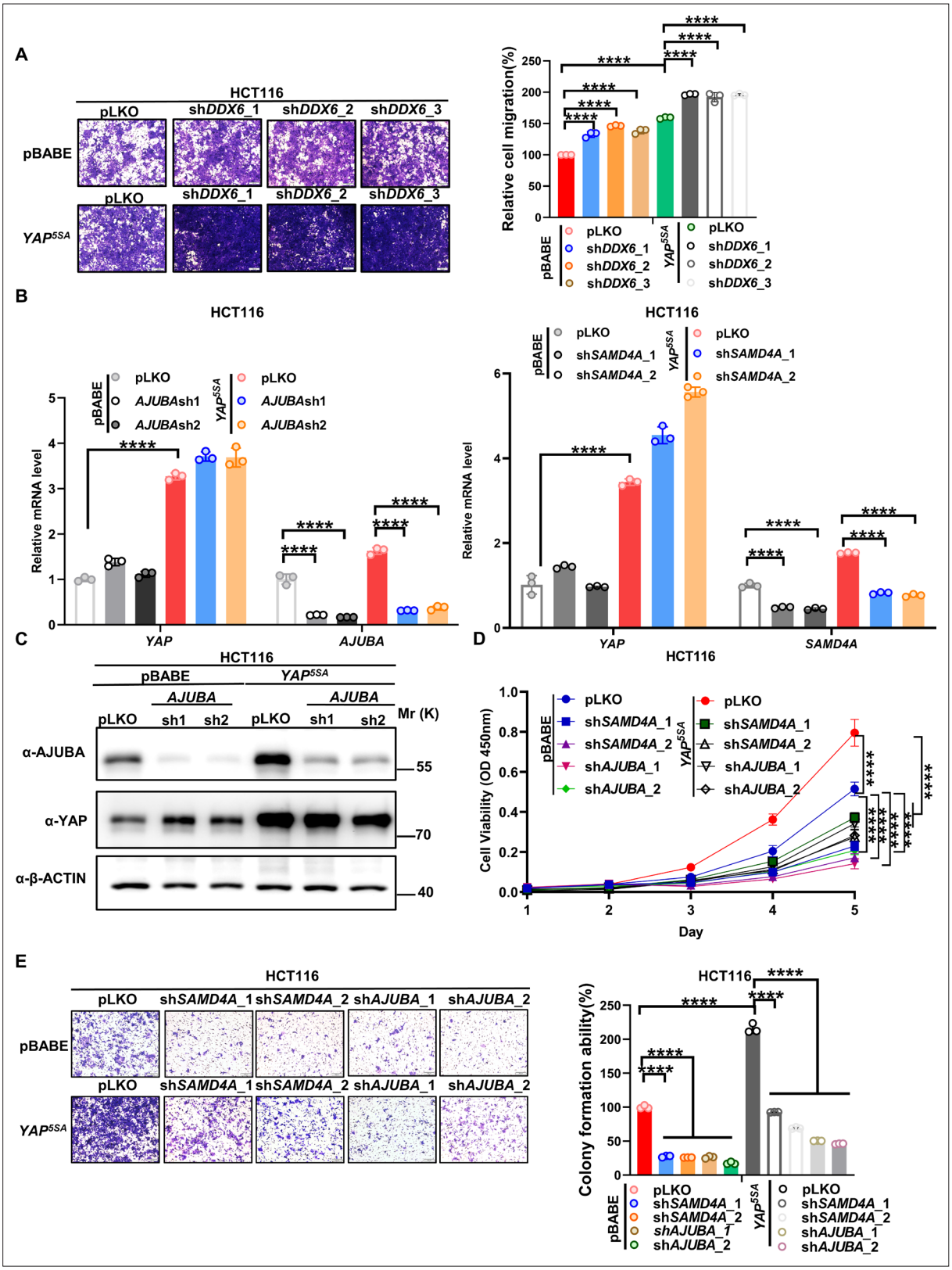

Figure 6—figure supplement 4. Knockdown of *AJUBA* or *SAMD4A* attenuates the oncogenic function of YAP in HCT116 cells. (**A**) Transwell assay of control HCT116 cells with or without knockdown of *DDX6* and HCT116 cells stably expressing YAP^{5SA} with or without knockdown of *DDX6*. n = 3 biologically independent samples per group. (**B, C**) qPCR (**B**) and western blot (**C**) analysis of the knockdown efficiency of *AJUBA* and *SAMD4A* in control HCT116 cells with or without knockdown of *AJUBA* or *SAMD4A* and stable YAP^{5SA} overexpression HCT116 cells with or without knockdown

Figure 6—figure supplement 4 continued on next page

Figure 6—figure supplement 4 continued

of *AJUBA* or *SAMD4A*. n = 3 biologically independent samples per group. (**D, E**) CCK8 proliferation (n = 5) (**D**) and Transwell (**E**) assays of control HCT116 cells with or without knockdown of *AJUBA* or *SAMD4A* and stable YAP^{5SA} overexpression HCT116 cells with or without knockdown of *AJUBA* or *SAMD4A*. One-way ANOVA (**A, B, E**) and two-way ANOVA (**D**) were performed to assess statistical significance in this figure. These data (**A, D, E**) are representative of three independent experiments.

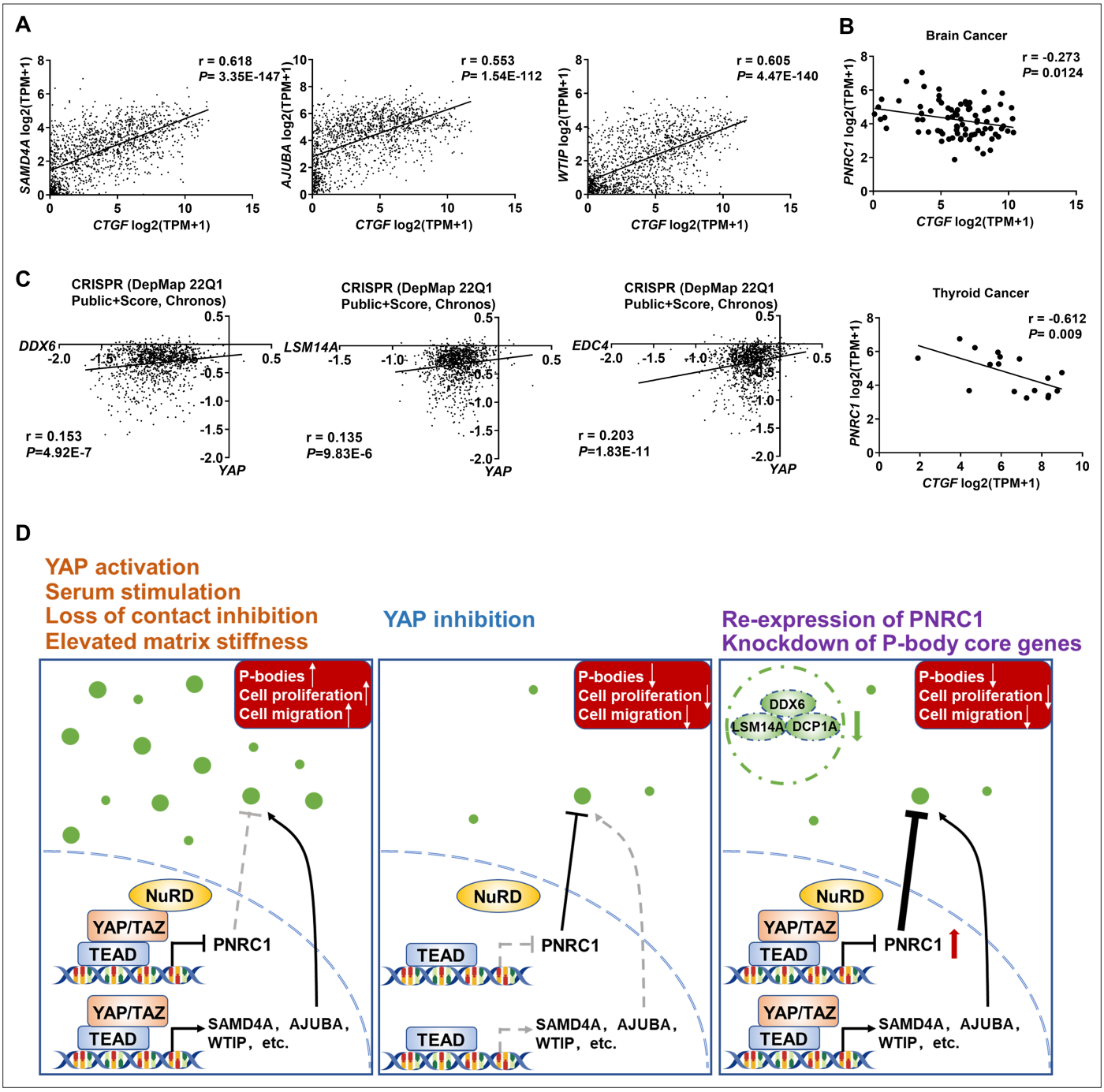

Figure 7. DepMap analysis reveals the co-dependencies of YAP/TEAD and P-body core genes in pancancer CRISPR screens. (**A**) Positive correlations between the mRNA levels of *CTGF* and *SAMD4A/AJUBA/WTIP* in 1393 cancer cell lines. (**B**) Negative correlation between the mRNA levels of *CTGF* and *PNRC1* in brain cancer cell lines (n = 83) and thyroid cancer cell lines (n = 17). (**C**) Positive correlations between the dependency scores of *YAP* and *DDX6/LSM14A/EDC4* in 1070 cancer cell lines. The Chronos dependency scores were extracted from the DepMap database. The negative Chronos score indicates decreased cell proliferation upon gene knockout. Pearson correlation analysis was used to assess statistical significance. (**D**) In response to serum stimulation or under loss of contact inhibition or reduced ECM stiffness, activation of YAP enhances the P-body formation to promote colorectal cancer (CRC) cell proliferation and migration. Disruption of P-bodies by overexpression of the tumor suppressor gene PNRC1 or knockdown of P-body core genes could attenuate the cell proliferation and migration induced by activation of YAP in CRC cells.

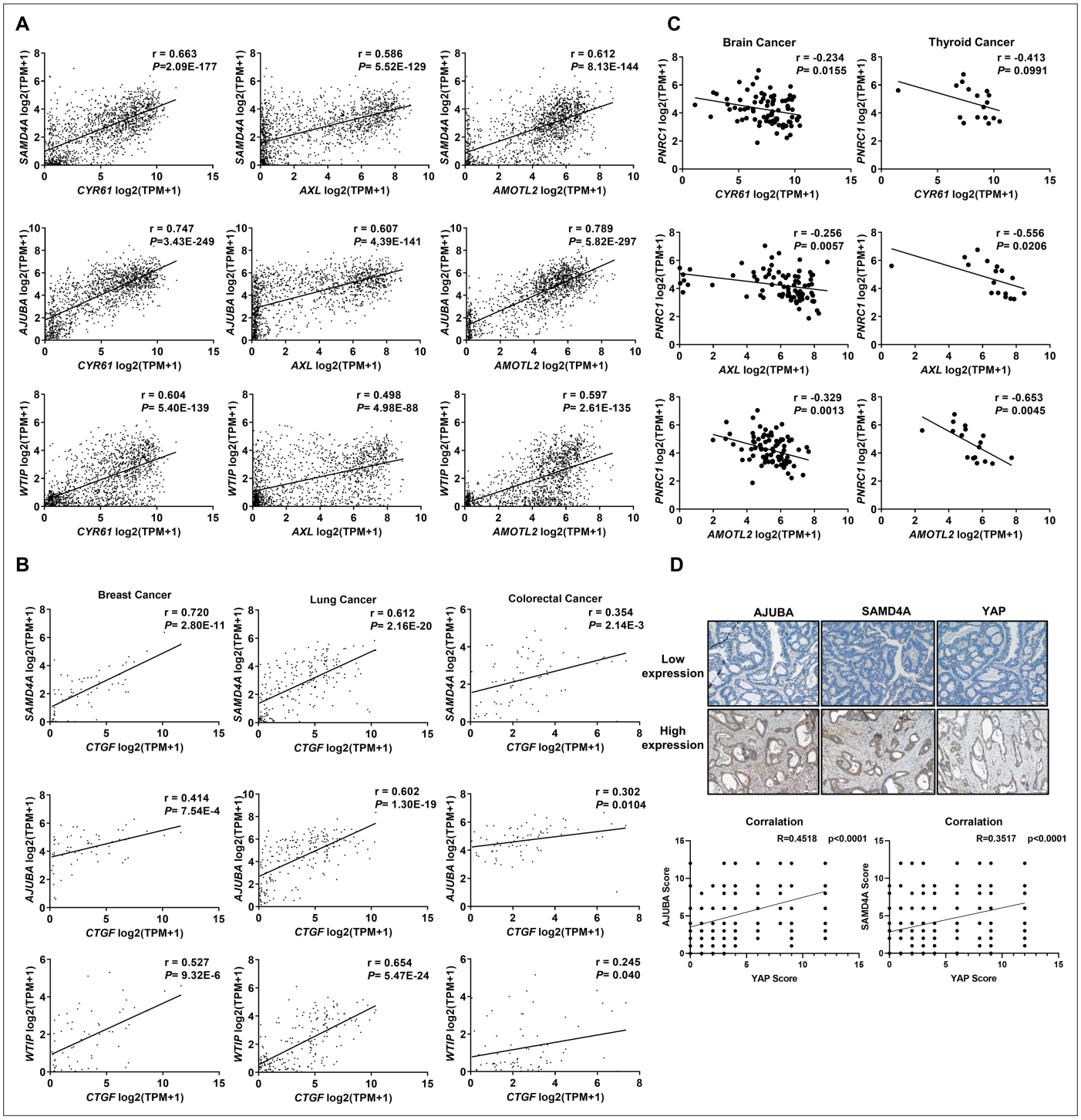

Figure 7—figure supplement 1. Correlation analysis of the expression of YAP canonical target genes and YAP-related P-body genes. (**A**) Positive correlations between the mRNA levels of YAP target genes (*CYR61*, *AXL*, and *AMOTL2*) and *SAMD4A/AJUBA/WTIP* in 1393 cancer cell lines. (**B**) Positive correlations between the mRNA levels of YAP target genes (*CTGF*) and *SAMD4A/AJUBA/WTIP* in brain cancer (n = 83), lung cancer (n = 207), and colorectal cancer (n = 71) cell lines. (**C**) Negative correlations between the mRNA levels of YAP target genes (*CYR61*, *AXL*, and *AMOTL2*) and *PNRC1* in brain cancer cell lines (n = 83) and thyroid cancer cell lines (n = 17). (**D**) IHC analysis of AJUBA, SAMD4A, and YAP protein expression in colorectal cancer tissues (n = 294). Pearson (**A–C**) and Spearman (**D**) correlation analysis was used to assess statistical significance.

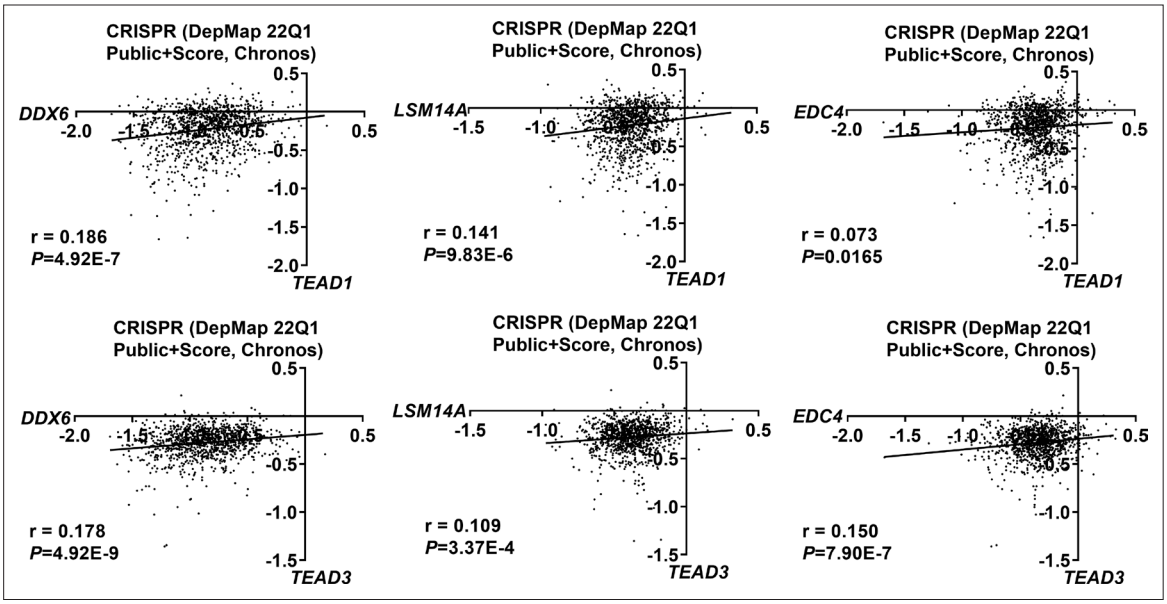

Figure 7—figure supplement 2. The *TEAD1/3* dependency scores are positively correlated with the *EDC4/DDX6/LSM14A* scores. Positive correlations between the dependency scores of TEAD1/3 and DDX6/LSM14A/EDC4 in 1070 cancer cell lines. The Chronos dependency scores were extracted from the DepMap database. The negative Chronos score indicates decreased cell proliferation upon gene knockout. Pearson correlation analysis was used to assess statistical significance.

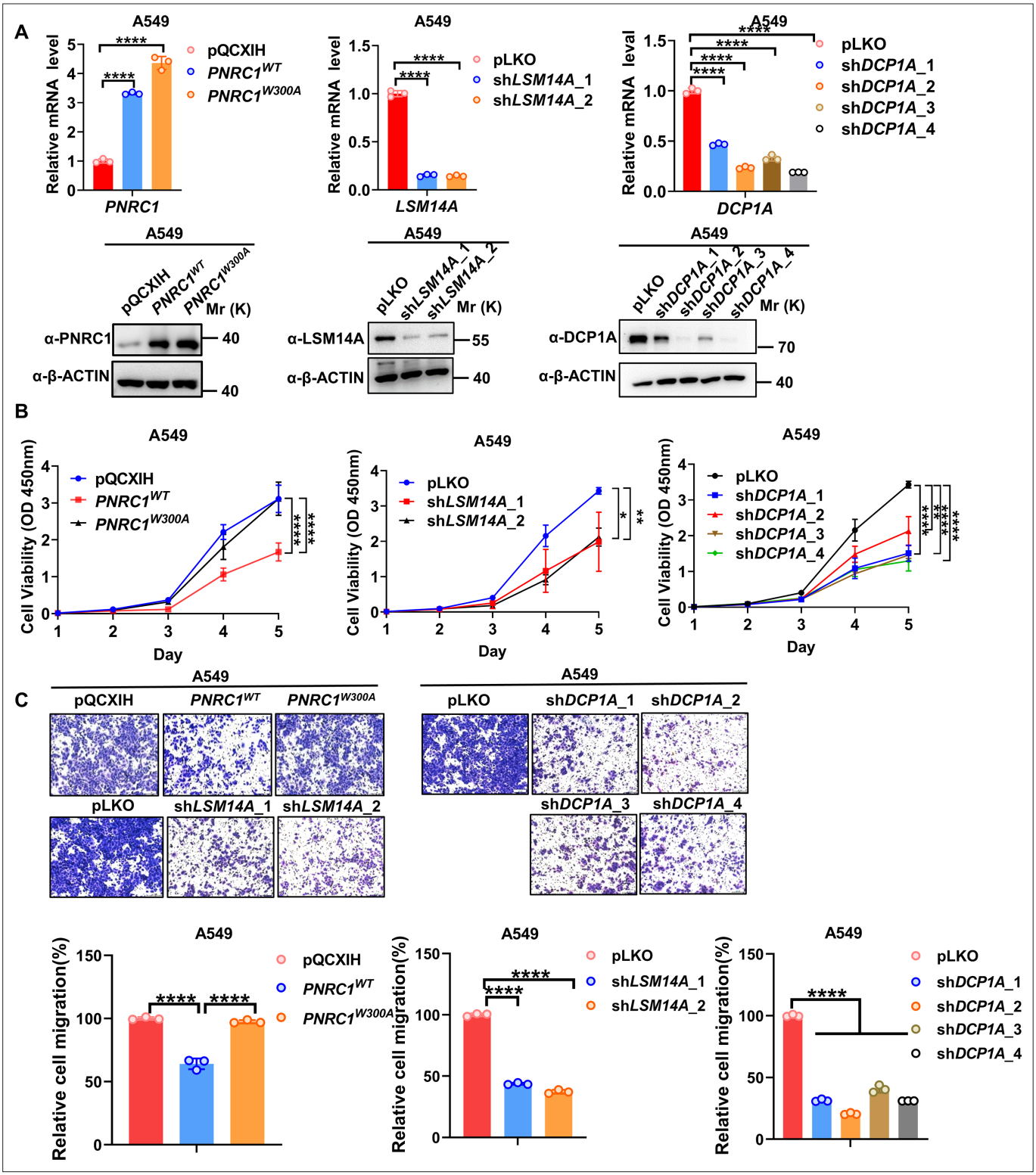

Figure 7—figure supplement 3. Knockdown of *DCP1A/LSM14A* and overexpression of PNRC1 suppress both cell proliferation and cell migration in A549 lung cancer cells. (**A**) qPCR and western blot analysis of the knockdown efficiency of *DCP1A / LSM14A* or PNRC1 overexpression in A549 cells stably expressing PNRC1^{WT}/PNRC1^{W300A} or with knockdown of *DCP1A* and *LSM14A*. (**B, C**) CCK8 proliferation (n = 5 for PNRC1 OE, n = 3 for knockdown of *DCP1A* and *LSM14A*) (**B**) and Transwell (**C**) assays of A549 cells stably expressing PNRC1^{WT}/PNRC1^{W300A} or with knockdown of *DCP1A* and *LSM14A*. Two-way ANOVA (**B**) and one-way ANOVA (**C**) were performed to assess statistical significance in this figure. These data (**B, C**) are representative of two independent experiment.

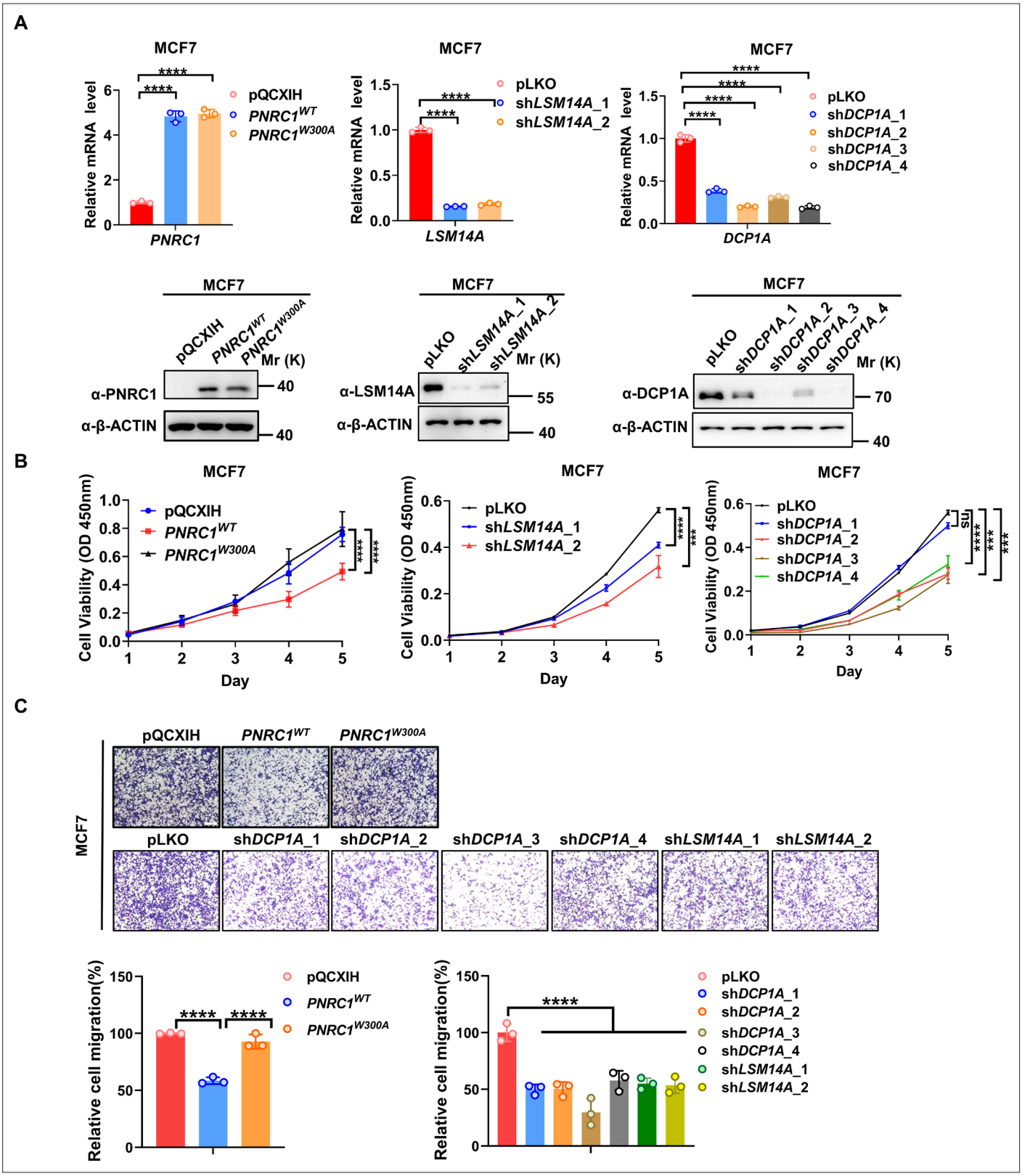

Figure 7—figure supplement 4. Knockdown of *DCP1A/LSM14A* and overexpression of PNRC1 suppress both cell proliferation and cell migration in MCF7 breast cancer cells. (**A**) qPCR and western blot analysis of the knockdown efficiency of DCP1A / LSM14A or PNRC1 overexpression in MCF7 cells stably expressing PNRC1WT/PNRC1W300A or with knockdown of DCP1A and LSM14A. (**B, C**) CCK8 proliferation (n = 6 for PNRC1 OE, n = 3 for knockdown of DCP1A and LSM14A) (**B**) and transwell (**C**) assays of MCF7 cells stably expressing PNRC1WT/PNRC1W300A or with knockdown of

Figure 7—figure supplement 4 continued on next page

Figure 7—figure supplement 4 continued

DCP1A and LSM14A. Two-way ANOVA (**B**) and one-way ANOVA (**C**) were performed to assess statistical significance in this figure. These data (**B, C**) are representative of 2 independent experiments.

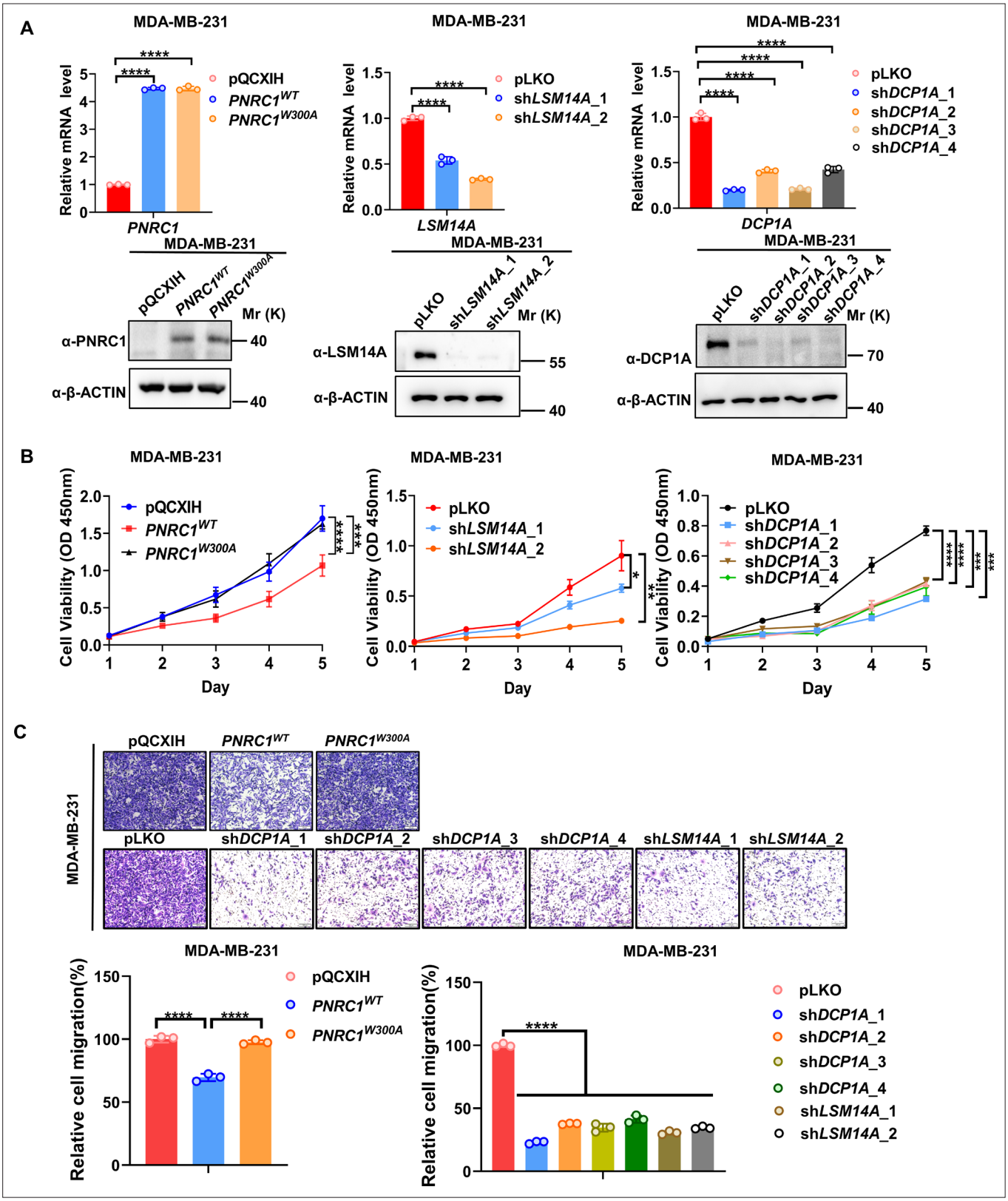

Figure 7—figure supplement 5. Knockdown of *DCP1A/LSM14A* and overexpression of PNRC1 suppress both cell proliferation and cell migration in MDA-MB-231 breast cancer cells. (**A**) qPCR and western blot analysis of the knockdown efficiency of DCP1A / LSM14A or PNRC1 overexpression in MDA-MB-231 cells stably expressing PNRC1WT/PNRC1W300A or with knockdown of DCP1A and LSM14A. (**B, C**) CCK8 proliferation (n = 6 for PNRC1 OE, n = 3 for knockdown of DCP1A and LSM14A) (**B**) and transwell (**C**) assays of MDA-MB-231 cells stably expressing PNRC1WT/PNRC1W300A or with

Figure 7—figure supplement 5 continued on next page

Figure 7—figure supplement 5 continued

knockdown of DCP1A and LSM14A. Two-way ANOVA (**B**) and one-way ANOVA (**C**) were performed to assess statistical significance in this figure. These data (**B, C**) are representative of 2 independent experiments.